White Matter Microstructure in Superior Longitudinal Fasciculus Associated with Spatial Working Memory Performance in Children

Martin Vestergaard[1*], Kathrine Skak Madsen[1,2,3*], William F. C. Baaré[1,2], Arnold Skimminge[1], Lisser Rye Ejersbo[4], Thomas Z. Ramsøy[1,3,5], Christian Gerlach[4], Per Åkeson[1], Olaf B. Paulson[1,2,3,6], and Terry L. Jernigan[1,2,3,7]

Abstract

■ During childhood and adolescence, ongoing white matter maturation in the fronto-parietal cortices and connecting fiber tracts is measurable with diffusion-weighted imaging. Important questions remain, however, about the links between these changes and developing cognitive functions. Spatial working memory (SWM) performance improves significantly throughout the childhood years, and several lines of evidence implicate the left fronto-parietal cortices and connecting fiber tracts in SWM processing. Here we report results from a study of 76 typically developing children, 7 to 13 years of age. We hypothesized that better SWM performance would be associated with increased fractional anisotropy (FA) in a left fronto-parietal network composed of the superior longitudinal fasciculus (SLF), the regional white matter underlying the dorsolateral pFC, and the posterior parietal cortex. As hypothesized, we observed a significant association between higher FA in the left fronto-parietal network and better SWM skills, and the effect was independent of age. This association was mainly accounted for by variability in left SLF FA and remained significant when FA measures from global fiber tracts or right SLF were included in the model. Further, the effect of FA in left SLF appeared to be mediated primarily by decreasing perpendicular diffusivity. Such associations could be related to individual differences among children in the architecture of fronto-parietal connections and/or to differences in the pace of fiber tract development. Further studies are needed to determine the contributions of intrinsic and experiential factors to the development of functionally significant individual differences in fiber tract structure. ■

INTRODUCTION

Spatial working memory (SWM) capacity develops throughout childhood and adolescence (Conklin, Luciana, Hooper, & Yarger, 2007; De Luca et al., 2003). Working memory is the ability to maintain and manipulate information relevant for the task at hand (Baddeley, 1981). Executive functions like working memory are considered essential for performing goal-oriented behaviors, and SWM deficits have been associated with behavioral disorders in children such as autism and attention deficit/hyperactivity disorder (ADHD) (Corbett, Constantine, Hendren, Rocke, & Ozonoff, 2009; Goldberg et al., 2005; Westerberg, Hirvikoski, Forssberg, & Klingberg, 2004). Studies of SWM have consistently implicated several brain regions as contributing to on-line maintenance and manipulation of spatial information. The dorsolateral pFC (DLPFC) and the posterior parietal cortex (PPC) have been linked to SWM functions (Van Asselen et al., 2006; Koch et al., 2005; Klingberg, Forssberg, & Westerberg, 2002). Lesions applied to the pFC (principal sulcus) in the macaque monkey cause profound deterioration of SWM performance (Funahashi, Bruce, & Goldmanrakic, 1993; Goldman & Rosvold, 1970). In human patients, SWM deficits have been associated with frontal lesions in the right (Van Asselen et al., 2006; Owen, Morris, Sahakian, Polkey, & Robbins, 1996) and the left hemisphere (du Boisgueheneuc et al., 2006; Owen et al., 1996). TMS studies have shown that stimulation of DLPFC and PPC in either the right or the left hemisphere disrupts SWM performance (Koch et al., 2005; Oliveri et al., 2001; Muri et al., 2000). These findings have been corroborated by single cell recordings in rhesus monkeys, demonstrating that SWM performance is related to electrophysiological activity in the principal sulcus (DLPFC) and PPC (Takeda & Funahashi, 2007; Chafee & Goldman-Rakic, 1998) and that the pattern of task-related activity in the principal sulcus matches that in the PPC during performance of an

[1]Copenhagen University Hospital, Hvidovre, Denmark, [2]Center for Integrated Molecular Brain Imaging, Copenhagen, Denmark, [3]University of Copenhagen, Denmark, [4]University of Aarhus, Copenhagen, Denmark, [5]Copenhagen Business School, Denmark, [6]Copenhagen University Hospital, Rigshospitalet, Denmark, [7]University of California, San Diego
*Contributed equally to this work.

SWM task (Chafee & Goldman-Rakic, 1998). Moreover, numerous fMRI and PET studies have revealed activation foci in prefrontal areas and PPC during SWM performance. The activation foci in prefrontal regions have been observed in both right and left DLPFC, and whether SWM is lateralized remains an issue of debate (Lycke, Specht, Ersland, & Hugdahl, 2008; Srimal & Curtis, 2008; Leung, Oh, Ferri, & Yi, 2007; Owen, McMillan, Laird, & Bullmore, 2005). Overall, the findings suggest that functions of DLPFC and PPC are important for SWM functioning. Studies of the rhesus monkey cortex confirm that the DLPFC and PPC have reciprocal connections within the major axon bundle of the superior longitudinal fasciculus (SLF) (Petrides & Pandya, 2006; Cavada & Goldman-Rakic, 1991).

Structural MRI studies have revealed gradual increases of white matter volume and apparent thinning of cortex during childhood and adolescence. Both gray and white matter exhibit protracted trajectories of developmental change that vary across different cerebral regions. Among the latest developing regions are portions of parietal and pFC (Sowell et al., 2004; Sowell, Trauner, Gamst, & Jernigan, 2002; Paus et al., 2001; Giedd et al., 1999; Jernigan, Trauner, Hesselink, & Tallal, 1991), and ongoing myelination of connecting fiber tracts between these regions is likely to relate to these cortical changes. However, conventional structural MRI provides only limited information about fiber tract structure.

Age-related change in microstructure of white matter during childhood and adolescence is measurable using diffusion tensor imaging (DTI) (Lebel, Walker, Leemans, Phillips, & Beaulieu, 2008; Eluvathingal, Hasan, Kramer, Fletcher, & Ewing-Cobbs, 2007; Snook, Paulson, Roy, Phillips, & Beaulieu, 2005). DTI measures properties of the diffusion of water in the brain. Within white matter, the axonal membrane and the surrounding myelin hinder diffusion perpendicular to the fiber tracts relative to diffusion parallel to the tracts, causing anisotropic diffusion (Beaulieu, 2002). Fractional anisotropy (FA) is a measure of the degree of elongation of the diffusion tensor (Basser, Mattiello, & LeBihan, 1994). FA, perpendicular diffusivity ($\lambda_\perp$), and parallel diffusivity ($\lambda_\parallel$) are estimated by fitting the diffusion measurements of each voxel to the diffusion tensor model (Beaulieu, 2002; Basser et al., 1994). DTI studies in young children have consistently shown age-related increases in FA associated with a disproportionate decrease in $\lambda_\perp$ relative to $\lambda_\parallel$, possibly related to ongoing myelination and increases in fiber density (Lebel et al., 2008; Eluvathingal et al., 2007; Snook et al., 2005). Furthermore, FA measures from different white matter fiber tracts exhibit variable developmental trajectories (Lebel et al., 2008), with FA in some approaching adult levels early and others not until after adolescence.

The relationship between age-related changes in the microstructural properties of white matter and the concurrent development of cognitive functions in children is still poorly understood, although a few studies suggest associations between FA values in white matter and performance on cognitive tasks (Madsen et al., 2010; Niogi & McCandliss, 2006; Nagy, Westerberg, & Klingberg, 2004). To date, one research group has examined associations between white matter FA and SWM performance in children and adolescents. Nagy et al. (2004) studied 23 children between 7 and 18 years of age, with an SWM task that required the children to remember the positions in a 4×4 spatial grid of sequences of red circles. DTI images were analyzed using a voxel-based analysis to identify regions exhibiting an association between FA and SWM performance. The investigators found that better SWM performance was correlated with increased FA values in, among other regions, a left inferior frontal cluster and a left fronto-parietal cluster; however, after adjusting for age, only the left inferior frontal cluster remained significant. Furthermore, in the same group of children, the variability in FA in the left fronto-parietal cluster that exhibited a relationship to SWM performance was also positively correlated with SWM-related fMRI activity in the left inferior parietal lobe and left superior frontal sulcus (Olesen, Nagy, Westerberg, & Klingberg, 2003). Interestingly, in one fMRI study of adolescents, age-related increases in SWM-related brain activation were observed in left prefrontal areas as well as in bilateral posterior parietal areas (Schweinsburg, Nagel, & Tapert, 2005).

In summary, there is strong evidence to implicate DLPFC and PPC in SWM functions, and DTI studies have shown that during childhood and adolescence, FA increases can be observed in the SLF, the major fiber tract connecting these areas (Lebel et al., 2008). SWM functions show age-related improvement across childhood and adolescence (Conklin et al., 2007), and limited evidence available from a study of children and adolescents suggests that FA variability in fronto-parietal white matter regions of the left hemisphere is associated with variability among children in their SWM skills. Because SWM performance and FA in white matter tracts are both known to increase with age in children, such associations between these two measures within a group of children of different ages could arise simply because of their association with chronological age. Indeed, in the study by Nagy et al. (2004), some of the associations between FA and SWM performance were substantially reduced when age was controlled. Of course, this could indicate that age-related increase in FA has a direct relationship with developing SWM functions, and thus controlling for age reduces the correlation. However, it could also indicate that factors not causally linked to chronological age, for example, years practicing SWM skills, mediate the apparent relationship between FA and SWM performance. In other studies of school-aged children, clear evidence has emerged for relationships between white matter FA and behavioral differences (e.g., on reading, verbal working memory, and inhibitory tasks) that remained after controlling for the age of the children (Madsen et al., 2010; Niogi & McCandliss, 2006). These associations suggest that the structure of brain fiber tracts may be related to individual differences among children that occur even among

children of similar age and may either be related to stable differences in neural architecture or to differences in the age trajectories of biological maturation of fiber tracts.

In the present study, we were interested in the degree to which FA variability in a fronto-parietal network consisting of SLF, DLPFC, and PPC could be linked to individual differences in SWM performance within a large group of 76 typically developing children between the ages of 7 and 13 years. Given the consistent evidence from earlier studies of SWM in children and adolescents that a left-sided neural system is implicated in the development of SWM skills, we hypothesized that FA in the left hemisphere SLF and in the white matter underlying the DLPFC and the PPC would account for significant variability in SWM performance, after accounting for any association mediated by chronological age. Follow-up analyses were planned to estimate the relative contributions of the three ROI measures to the prediction of SWM performance and to further examine the anatomical specificity of the effects by including as covariates either an estimate of global white matter FA or an FA in the corresponding right hemisphere ROI. The parallel and perpendicular diffusivities were also examined to further explore the nature of significant associations with FA.

METHODS

Subjects

Ninety-two typically developing children aged 7 to 13 years (mean ± *SD*: age = 10.0 ± 1.7 years, 53 girls, 39 boys) from three schools (first to sixth graders) in the Copenhagen area participated in the study. All children assented to the procedures, and informed written consent was obtained from the parents/guardians of all subjects before participation after oral and written explanation of the study aims and study procedures. The study was approved by the local Danish Committee for Biomedical Research Ethics (H-KF-01-131/03) and conducted in accordance with the Declaration of Helsinki. Sixteen of the participating subjects (9 girls, 7 boys) were subsequently excluded as described in the Image evaluation section. Thus, 76 subjects were included in the analyses reported here (mean ± *SD*: age = 10.1 ± 1.6 years, 44 girls, 32 boys). According to parent reports, no subjects had any known history of neurological or psychiatric disorders or significant brain injury. There were no significant differences between the included and the excluded subjects on age, sex, parental education, or handedness (as assessed with the Edinburgh Handedness Inventory). Demographic data from the included subjects are presented in Table 1.

SWM Task

SWM was assessed using the Cambridge Neuropsychological Test Automated Battery (CANTAB; Cambridge Cognition Ltd., Cambridge, UK). The CANTAB SWM task is computerized and was administered using a Paceblade touch screen computer. Subjects are shown a display containing *N* colored boxes and told that a blue token is hidden inside one of the boxes. Subjects must find the hidden token by touching the boxes until the token is located. The subject then moves the blue token to a column to the right of the display and must start a new search of the same array of boxes for a token now hidden in one of the previously empty boxes. This continues until a blue token has been located in each of the boxes (positions). The number of boxes in the array is then gradually increased from three to eight boxes. The trials containing only three boxes are used as control trials. The color and the position of the boxes vary from trial to trial to discourage the use of stereotyped search strategies. The primary behavioral outcome measure is the "between-errors" score, which is a measure of the number of times the subject returns to a box in which a blue token has already been located during that trial.

Image Acquisition

All subjects were scanned using a 3-T Siemens Magnetom Trio MR scanner (Siemens, Erlangen, Germany) with an eight-channel head coil (Invivo, Orlando, FL). Subjects were scanned the same day as SWM was assessed. All scans were acquired aligned parallel to the AC–PC line. Diffusion-weighted (DW) images of the whole brain were acquired using a twice-refocused balanced spin echo sequence that minimized eddy current distortion (Reese, Heid, Weisskoff, & Wedeen, 2003). Ten non-DW images ($b = 0$) and 61 DW images, encoded along independent collinear diffusion

Table 1. Demographic Data for the Included Subjects

	First/Second Graders	*Third/Fourth Graders*	*Fifth/Sixth Graders*	*All Subjects*
Age (mean ± *SD*)	8.2 ± 0.5	10.1 ± 0.4	12.2 ± 0.4	10.1 ± 1.6
Sex (female/male)	14/10	16/13	14/9	44/32
Handedness (right/left)	21/3	24/5	21/2	66/10
Parents' average years of education (mean ± *SD*)	14.0 ± 1.7	13.4 ± 2.0	13.7 ± 2.0	13.7 ± 1.9

Children enrolled in the study were scanned either in the months just before (when in first, third, or fifth grade) or just after (when in second, fourth, or sixth grade) the summer school holiday.

gradient orientations (Cook et al., 2006; Jansons & Alexander, 2003), were acquired with a *b* value of 1200 s/mm^2 (repetition time [TR] = 8200 msec, echo time [TE] = 100 msec, field of view [FOV] = 220 × 220 mm^2, matrix = 96 × 96, GRAPPA: acceleration factor = 2, number of reference lines = 48, 61 perpendicular slices with no gap, 2.3 × 2.3 × 2.3 mm^3 voxels, NEX = 1, acquisition time = 9.50 min). A gradient-echo-based field map sequence (TR = 530 msec, TE[1] = 5.19 msec and TE[2] = 7.65 msec, FOV = 256 × 256 mm^2, matrix = 128 × 128, 47 perpendicular slices with no gap, voxel size = 2 × 2 × 3 mm^3, NEX = 1, acquisition time = 2.18 min) was acquired to correct geometric distortions caused by B0 magnetic field inhomogeneities. T_2-weighted images of the whole head were acquired using a 3-D turbo spin echo sequence (TR = 3000 msec, TE = 354 msec, FOV = 282 × 216 mm^2, matrix = 256 × 196, 192 sagittal slices, 1.1 mm^3 isotropic voxels, NEX = 1, acquisition time = 8.29 min) for generating brain masks.

Image Evaluation

All subjects' images were screened for neurological anomalies by an experienced neuroradiologist. Before image analysis and blind to behavioral data, the raw images from all subjects were visually checked to ascertain the quality of the data. As described earlier, on the basis of this inspection, 1 subject with incidental neurological findings, 3 subjects not completing the scanning session, and 12 subjects with significantly reduced image quality due to movement or susceptibility artifacts were excluded from further analysis.

Image Analysis

Images were preprocessed using pipelines implemented in Matlab, using mainly SPM5 routines. DW images were oriented to the Montreal Neurological Institute (MNI) coordinate system and corrected for geometric distortions because of B_0 inhomogeneities and imaging gradient nonlinearities. At first, the mean b0 image was coregistered to the T_2-weighted image using a rigid transformation (six-parameter mutual information), after which all DW images were coregistered (no reslicing) to the mean b0 image. Next, all coregistered images were corrected for geometric distortion using both the acquired B_0 field map (Andersson, Hutton, Ashburner, Turner, & Friston, 2001) and the scanner-specific maps of gradient nonlinearities (Jovicich et al., 2006). All images were resliced using trilinear interpolation. Note that this procedure involves only one interpolation step. The diffusion gradient orientations were adjusted to account for any rotation applied during registration. The diffusion tensor was fitted using the RESTORE algorithm with a noise standard deviation of 30 (Chang, Jones, & Pierpaoli, 2005) implemented in Camino (Cook et al., 2006), and FA and diffusivity parallel ($\lambda_\parallel = \lambda_1$) and perpendicular ($\lambda_\perp = (\lambda_2 + \lambda_3) / 2$) to the principal diffusion direction were calculated. A brain mask on the basis of the T_2-weighted image was automatically created using SPM5 segmentation routines and morphological operations and applied to the FA and diffusivity images.

Intersubject Spatial Normalization of Fiber Tracts

In the present study, we extracted FA and diffusivity measures from specific ROIs for each subject to test our hypotheses. Spatial normalization and alignment of fiber tracts across children were achieved by means of the tract-based spatial statistics (TBSS) module (Smith et al., 2006), part of FSL 4.1.0 (Smith et al., 2004). At first, subjects' FA images were aligned into a common space using the nonlinear registration tool FNIRT (Andersson, Jenkinson, & Smith, 2007). A study-specific target, the group's most representative FA image, was then identified after nonlinearly registering each subject's FA image to every other subject's FA image. Next, the target FA image was aligned to MNI space using affine registration, and subsequently the entire aligned data set was transformed into 1 mm^3 MNI space. After this, a cross-subject mean FA image was created and thinned to create a study-specific mean FA skeleton, representing the centers of all tracts common to the group. The mean FA skeleton was thresholded at FA > 0.25 and contained 103,588 1 mm^3 interpolated isotropic voxels, corresponding to approximately one quarter of the voxels with FA greater than 0.25. Each subject's aligned FA image was then projected onto the mean skeleton by locating the highest local FA value in the direction perpendicular to the skeleton tracts and by assigning this value to the subject's skeleton. In addition, the nonlinear warps and the skeleton projections were applied to the $\lambda_\parallel$ and $\lambda_\perp$ data. Further, to generate a color-coded target FA map, the affine transformation generated when aligning the target FA image to MNI space was applied to the target's primary eigenvector ($\mathbf{v}_1$) image using the vecreg command in FSL.

Regions of Interest

ROIs were drawn onto a representation of the study-specific mean FA skeleton overlaid on the "study-representative" FA map. SLF, DLPFC, and PPC ROIs for the hypothesis tests were drawn in the left hemisphere and, for post hoc analyses, also in the right hemisphere (see Figure 1D). The borders of the DLPFC and PPC ROIs were located using a human brain atlas (Duvernoy, 1999) and were drawn using anatomical information visible in the study-specific target FA map. The SLF ROI was drawn using the target's color-coded FA map and was defined in accordance with the MRI Atlas of Human White Matter (Mori, Wakana, Nagae-Poetscher, & van Zijl, 2005; for a comparison example between a gray-scaled FA map and a color-coded FA map from the same coronal slice, see Figure 1B and E).

The posterior border of the DPLFC ROI defined the anterior border of the SLF, and the anterior border of

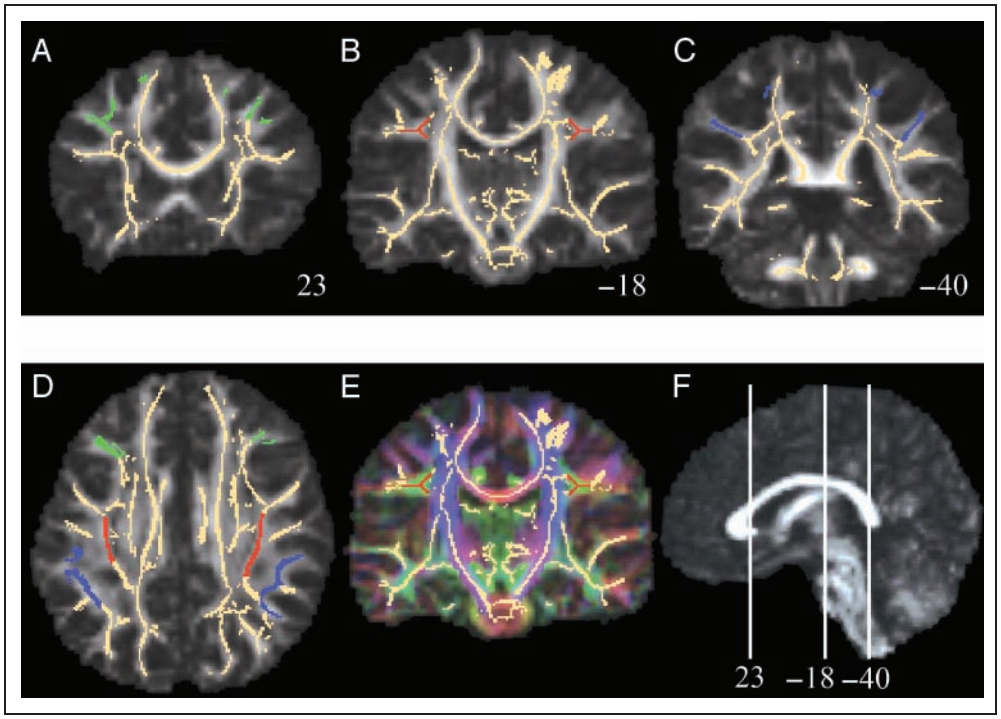

Figure 1. Abbreviations: DLPFC = dorsolateral pFC, PPC = posterior parietal cortex, SLF = superior longitudinal fasciculus. The slices A–E depict the mean FA skeleton (light-yellow) overlaid on the target FA image. (A) Coronal slice of DLPFC in green; (B) coronal slice of SLF in red; (C) coronal slice of PPC in blue; (D) axial slice of left- and right-sided DLPFC, SLF, and PPC ROIs. (E) Coronal slice of SLF in red (for a comparison, see Figure 2B) displayed on the target color-coded FA map showing the direction of the primary eigenvector in colors (anterior–posterior direction in green, superior–inferior direction in blue, and left–right in red). (F) Midsagittal image depicting the MNI coordinates of coronal slice A, B, C, and E. The images are displayed according to neurological convention (left is left).

the PPC ROI defined the posterior border of the SLF. The SLF ROI only included white matter voxels with anterior–posterior oriented primary eigenvectors (green in the color-coded FA map in Figure 1E). The left SLF ROI contained 745 voxels, and the right SLF ROI contained 736 voxels.

The DLPFC ROI included the white matter underlying the superior frontal gyrus and the middle frontal gyrus (see Figure 1A). The anterior border of the DLPFC was indicated by low FA values demarcating the border of the anterior inferior frontal sulcus to exclude the frontal pole. The posterior border was delineated at the precentral sulcus. The medial border of the middle frontal gyrus was delineated according to the depth of the superior and inferior frontal sulci and the direction of the skeleton (see Figure 1A). The superior frontal gyrus was only drawn when a lateral part of the skeleton could be distinguished. The left DLPFC ROI contained 1506 voxels, and the right DLPFC ROI contained 1384 voxels.

The PPC ROI included the white matter underlying the superior parietal lobule and the inferior parietal cortex (IPC) (see Figure 1C). The anterior boundary of the PPC ROI was defined by the postcentral sulcus. The posterior border of the superior parietal lobule was defined by the parieto-occipital sulcus, whereas the posterior boundary of the IPC was defined by the angular sulcus/secondary intermediate sulcus. The inferior border of the IPC was defined by the sylvian fissure and medially by the circular insular sulcus. The medial border of the IPC was defined by the lateral boundaries of the SLF ROI (see Figure 1C). The left PPC ROI contained 1131 voxels, and the right PPC ROI contained 1365 voxels.

Mean FA and parallel ($\lambda_{\parallel}$) and perpendicular ($\lambda_{\perp}$) diffusivity values from all six ROIs and the whole skeleton (as an estimate of global white matter FA) were extracted for each subject for statistical analyses.

Statistical Analysis

Statistical analyses were done using the Statistical Package for the Social Sciences for Windows (Version 18.0; SPSS Inc., Chicago, IL). Multiple linear regression models were used to predict SWM performance. Because SWM performance is measured in number of errors (i.e., between errors = the number of times the subject returns to a box in which a blue token previously has been located), better SWM performance should correlate negatively with increasing age or FA. The major hypothesis was that increased FA in a left fronto-parietal network would contribute significantly to the prediction of better SWM performance (i.e., less "between errors") after adjusting for effects of age. This hypothesis was tested with a hierarchical regression analysis (Cohen & Cohen, 1983) in which at the first step only age predicted the SWM error score and at the second step the three left ROI FA measures were entered simultaneously as predictors. The change in R^2 attributable to the set of variables was then tested for significance. A p value less than .05 was considered significant for the primary hypothesis that the set of ROI FA measures would significantly improve the prediction of SWM

Table 2. Between-Errors SWM and FA Measures of the ROIs

	Minimum	*Maximum*	*Mean ± SD*
SWM between errors	2	62	28.16 ± 15.3
Left SLF FA	0.415	0.568	0.495 ± 0.03
Left DLPFC FA	0.350	0.461	0.402 ± 0.02
Left PPC FA	0.341	0.469	0.408 ± 0.03
Right SLF FA	0.407	0.554	0.476 ± 0.031
Right DLPFC FA	0.353	0.474	0.409 ± 0.028
Right PPC FA	0.327	0.492	0.410 ± 0.032

DLPFC = dorsolateral pFC; PPC = posterior parietal cortex; SLF = superior longitudinal fasciculus.

performance after adjusting for age. Follow-up regression analyses were planned to examine the anatomical specificity of the results by including as covariates either the whole skeleton FA or the corresponding right hemisphere ROI FA in a multiple linear regression model, also adjusting for age as in the primary analyses. Planned follow-up analyses further examined the parallel ($\lambda_{\parallel}$) and the perpendicular ($\lambda_{\perp}$) diffusivities to explore the specific effects of the diffusivities by following the same statistical analysis protocol as for the FA data. Collinearity (multicollinearity) between the predictors was assessed for all regression models.

Finally, an effect-size map is presented to provide further (more qualitative) information about variation across the white matter skeleton in the effect size relating FA to SWM performance (Jernigan, Gamst, Fennema-Notestine, & Ostergaard, 2003). The effect-size map is based on *t* maps of the correlation between FA and SWM performance (i.e., between errors) after controlling for age; however, the sign of the correlations is reversed so that high FA and better SWM performance (i.e., fewer errors) are shown in warm colors (red to yellow). The *t* map was generated using the Monte Carlo permutation test, with 10,000 permutations implemented in the randomize program within FSL (Nichols & Holmes, 2002).

RESULTS

The distributions of the between-errors score from the SWM task and of the FA measures for the six ROIs are presented in Table 2. For comparison, four regression subplots are presented in Figure 2 to show the results from linear regression analyses of SWM performance as a function of age (Figure 2A), left SLF as a function of age (Figure 2B),

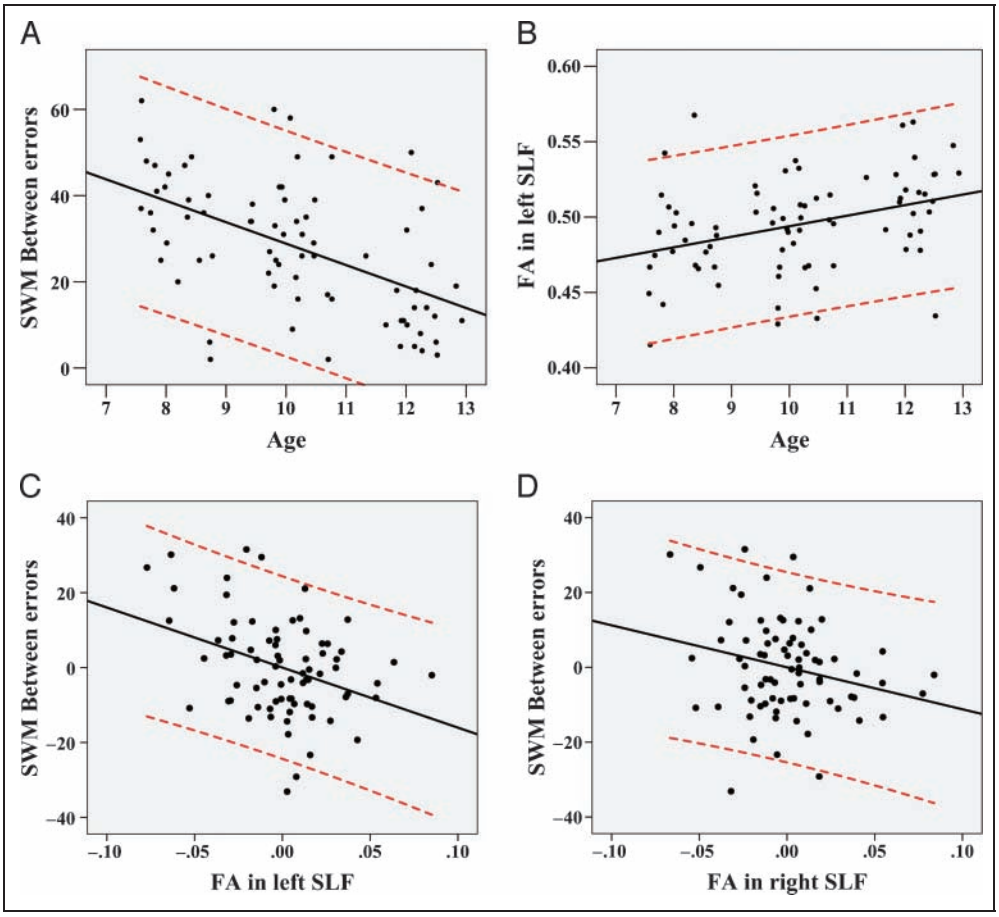

Figure 2. Linear regression plots of (A) SWM (between errors) as a function of age (Model 1). (B) FA in left SLF as a function of age. Partial regression plots of (C) SWM (between errors) as a function of FA in left SLF, adjusted for age and (D) SWM (between errors) as a function FA in right SLF, adjusted for age. We note that the right SLF FA is *not* a significant predictor of SWM "between errors" with left SLF included in the model (Table 4, Model 5) after controlling for age. The red dotted lines correspond to the 95% confidence interval for the individual data points.

Table 3. Hierarchical (A Priori) Multiple Linear Regression Models Predicting SWM Errors

		Left DLPFC FA		*Left PPC FA*		*Left SLF FA*		*Age*			
	R^2	β	p	β	p	β	p	β	p	R^2 *Change*	p
Model 1	.281							−.530	8.32×10^{-7}		
Model 2	.384	.092	.419	−.057	.623	−.330	.003	−.432	.0001	.103[a]	.011[a]

Each row in the table represents a separate regression model. R^2 is given in the leftmost column. For each variable included in the model, the slope (β) and the significance level (p) are given. The rightmost columns contain R^2 change and associated significance level. Here, R^2 change refers to the amount R^2 increases or decreases when variables are added to a model. DLPFC = dorsolateral pFC; PPC = posterior parietal cortex; SLF = superior longitudinal fasciculus.

[a]R^2 additionally explained by Model 2 as compared with Model 1, which only includes age as a predictor.

partial regression of SWM performance as a function of left SLF FA adjusted for age (Figure 2C), and partial regression of SWM performance as a function of right SLF FA adjusted for age (Figure 2D).

The results of the multiple linear regression analyses are summarized in Table 3 and Table 4. Each row of the tables provides the result of a separate, planned model predicting SWM scores. Age was significantly and negatively associated with SWM performance (between errors) (Model 1, Figure 2A). As hypothesized, increased FA in the left fronto-parietal network contributed significantly to the prediction of better SWM performance after adjusting for age (Model 2). Inspecting the three regression coefficients for the left ROI FA measures in Model 2 (the hierarchical stepwise regression analysis) revealed that only left SLF made a significant contribution whereas left DLPFC and left PPC contributions were negligible. Given this, follow-up models focused only on the SLF ROI measures.

The first follow-up analysis (Model 3) was performed to confirm the strong contribution of left SLF FA (alone) to the prediction of SWM performance, after controlling for age. Next, we confirmed that when including the whole skeleton FA in the model, only left SLF FA reached significance (Model 4), suggesting that the association between SWM and left SLF FA was not mediated by global increases in FA. Then, to further examine the laterality of the effect, we included in the model the measure of FA in the corresponding right hemisphere SLF ROI. Again, only left SLF FA remained significant (Model 5). We note, however, that right SLF FA was a significant predictor of SWM errors without left SLF in the model (not shown in the table), after controlling for age ($R^2 = .324$, $\beta = -.224$, $p = .036$). In additional post hoc analyses predicting SWM errors, neither right DLPFC FA nor right PPC FA made a significant contribution after controlling for age.

Additional exploratory analyses of the eigenvalues revealed that left SLF $\lambda_\parallel$ did not show a significant relationship with SWM performance after controlling for age. However, SWM performance was significantly and positively associated with left SLF $\lambda_\perp$ after adjusting for age (Model 6), and this effect remained significant when entering whole skeleton $\lambda_\perp$ (Model 7) or right SLF $\lambda_\perp$ (Model 8) as covariates.

Collinearity diagnostics were performed for all of the regression models, with no model exhibiting a Tolerance

Table 4. Follow-up Multiple Linear Regression Models Predicting SWM Errors

		Left SLF ROI		*Age*		*Whole Skeleton*		*Right SLF ROI*	
	R^2	β	p	β	p	β	p	β	p
FA									
Model 3	.378	−.334	.001	−.411	8.32×10^{-7}				
Model 4	.378	−.331	.008	−.410	.0002	−.004	.975		
Model 5	.379	−.364	.013	−.417	.0001			.043	.77
Perpendicular Diffusivity ($\lambda_\perp$)									
Model 6	.354	.303	.005	−.392	.0004				
Model 7	.356	.357	.028	−.400	.0004	−.072	.648		
Model 8	.370	.516	.008	−.410	.0003			−.251	.182

Each row in the table represents a separate regression model. R^2 is given in the leftmost column. For each variable included in the model, the slope (β) and the significance level (p) are given. SLF = superior longitudinal fasciculus.

value less than .20 or a variance inflation factor (VIF) higher than 5 (Models 2–5: tolerance = 0.405–0.871, VIF = 1.148–2.471; Models 6–8: tolerance = 0.242–0.795, VIF = 1.263–4.133).

Effect-size Map

The present study was designed to test a specific anatomical hypothesis about the relationship between FA in the connections of a left fronto-parietal network and variability in SWM performance in children. Therefore, neither a whole-brain, voxel-wise analysis of the effects (appropriately adjusted for test-multiplicity) nor a restricted voxel-based analysis with small volume correction was deemed appropriate for testing this a priori hypothesis. However, because the analysis we used produces estimates of the effect size at each voxel within the skeleton, we have provided a visualization of an effect-size map showing the association between FA and SWM performance adjusted for age (Figure 3). The map shows the distribution of t values in skeleton voxels and is presented to provide additional information about the anatomical distribution of associations between SWM performance and FA in the white matter. The contrast has been coded so that association of lower SWM errors (better performance) with higher FA yields positive t values, and increasing t values are shown in warm colors ranging from red to yellow. The map reveals some areas with apparent relationships between FA and SWM performance comparable with those in the left SLF, although it should be emphasized that these are uncorrected t values. The skeleton as a whole contained 103,588 voxels, of which 6788 voxels, or 6.5%, had associated t values greater than 1.99 (a value associated with an uncorrected $p < .05$). In contrast, within the combined left DLPFC, PPC, and SLF ROIs, 21.1% of the voxels had t values exceeding this value, and within the left SLF ROI alone, 43.5% of the t values exceeded this value. By comparison, only 11% of the t values in the right SLF ROI exceeded 1.99.

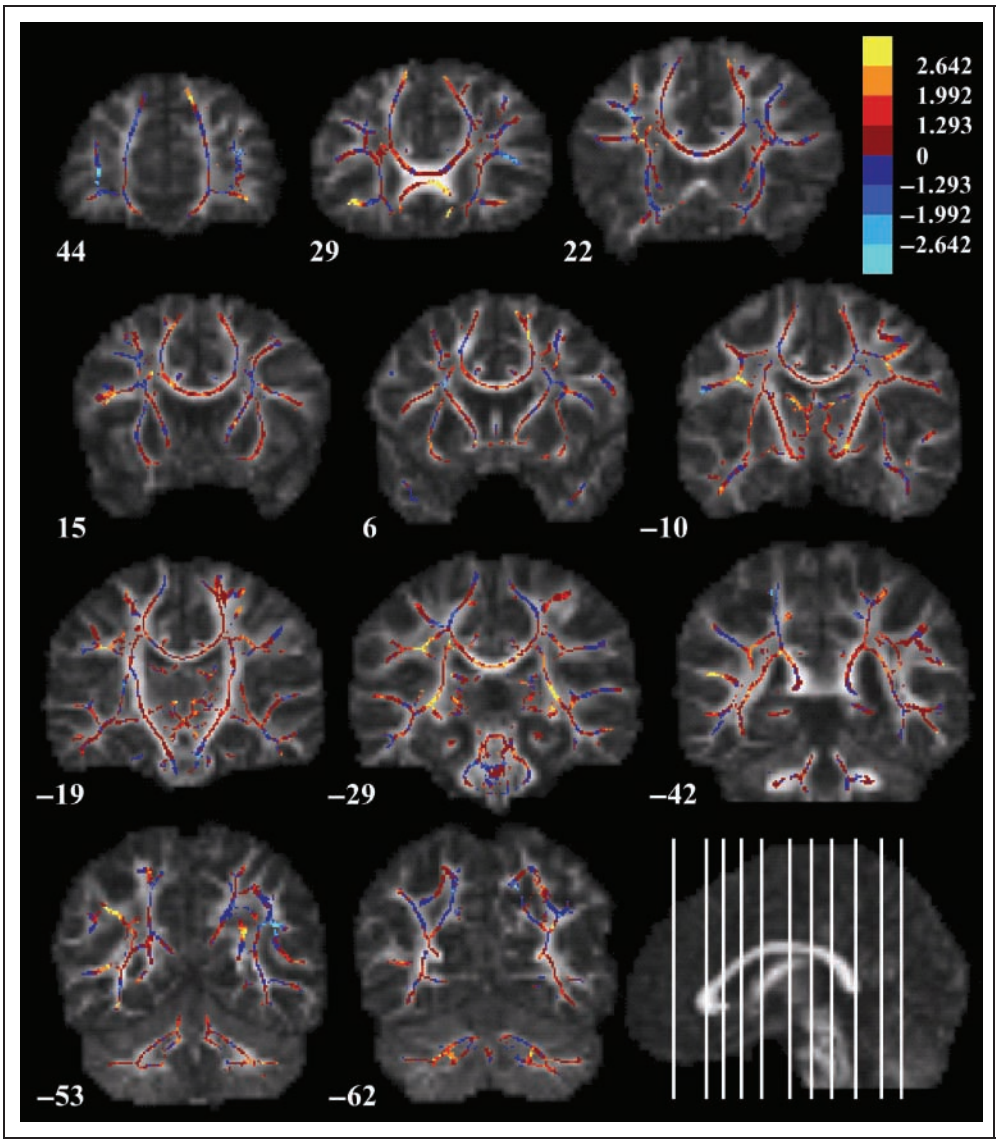

Figure 3. Effect-size map of the association between SWM performance and FA adjusted for age The effect-size map is overlaid on the target FA image. The color bar shows the color mapping of all skeleton voxels to the values of the t statistics ($t = 0 = p = 1$; $-1.293 > t > 1.293 = p < .2$; $-1.992 > t > 1.992 = p < .05$; $-2.642 > t > 2.642 = p < .01$). The MNI coordinates for the coronal images are displayed below each image. In the down-right corner, the MNI coordinates of the coronal slices are depicted on the midsagittal image with coronal slice 44 displayed to the far left and coronal slice −62 being displayed to the far right. The images are displayed according to neurological convention (left is left).

From the effect-size map several cluster of t values exceeding 2.64 were apparent. Among these was a cluster located in the genu of corpus callosum (Figure 3, coronal slice 29), a bilateral cluster comprising diverse fiber tracts such as inferior longitudinal fasciculus, inferior fronto-occipital fasciculus and posterior thalamic radiation (Figure 3, coronal slice −29) and a cluster part of which was contained in the left PPC ROI (Figure 3, coronal slice −53) in addition to a number of smaller clusters.

DISCUSSION

This study examined associations between SWM performance and properties of white matter microstructure in a left fronto-parietal network. As hypothesized, the results suggest that increased FA in left fronto-parietal connections exhibits a significant association with better SWM performance in children between the ages of 7 and 13 years, after adjusting for effects statistically attributable to age. Because both SWM abilities (Conklin et al., 2007) and FA in brain fiber tracts (Lebel et al., 2008) are known to increase in children over the age range from 7 to 13 years, a simple correlation between these measures could represent a nonspecific association attributable to unmeasured factors indexed by chronological age. For example, because height also increases in children over this age range, one might expect to find a simple correlation between height and SWM abilities within a group of children with varying ages, although few would infer that height has a direct relationship to cognitive functioning in children. One would also expect that the correlation between height and cognitive function would be substantially reduced after controlling for age statistically. Thus, we hypothesized that the association between FA in the left fronto-parietal network and SWM performance would remain significant after controlling for age; that is, that even among children of similar age, those with higher FA in a left fronto-parietal network would exhibit stronger SWM performance. Such a finding would be consistent with a relationship between structural connectivity in this network and individual differences in SWM abilities not attributable to age-related differences. This hypothesis was confirmed.

Several follow-up analyses were conducted to explore the nature of this association. We found that only FA in the ROI that included connecting fibers in left SLF could be shown to contribute significantly to the prediction of SWM performance (again, after controlling for age). We further examined the anatomical specificity of the association between SWM performance and fiber structure within the left SLF, that is, in the extent to which SWM exhibited a relatively specific relationship to FA in this fiber tract relative to other white matter regions. This is an important question because FA is known to increase during childhood concurrently in many fiber tracts (Lebel et al., 2008). However, the results of analyses including whole skeleton FA as a covariate suggest that the relationship between left SLF FA and SWM is not likely to be mediated by global white matter FA differences, which might occur because of individual differences in the phase or intensity of brain myelination per se.

We were not able to demonstrate a significant association between SWM ability and either of the FA measures from the left hemisphere superficial white matter ROIs (DLPFC or PPC) after controlling for age. These analyses may have been limited by low power or sensitivity. It is possible that the fibers within these segments of the tract skeleton were more mixed, that is, included more fibers from tracts other than the SLF, and thus FA in these ROIs may have been a less sensitive index of structural attributes in the targeted fronto-parietal association fibers. Longitudinal studies or studies with larger samples and/or more sensitive methods may still reveal a relationship between SWM ability and structural variability in segments of the left SLF that extend into these regions.

Our findings of an association of SWM performance with white matter structure in developing children extend initial findings from a previous DTI study of a much smaller group of children (Nagy et al., 2004). The previous study was performed using voxel-wise analyses and did not examine specific fiber tracts connecting fronto-parietal cortical regions. We used an ROI approach and focused specifically on segments of the white matter likely to contain fibers of the SLF. In the present study as well as in the study by Nagy et al. (2004), associations were observed between SWM performance and DTI parameters in left rather than right hemisphere tracts. These results are also consistent with prior fMRI studies that implicate the left hemisphere in SWM functions in children and adolescents (Schweinsburg et al. 2005; Olesen et al., 2003; Klingberg et al., 2002). However, the results of our analyses do not rule out the possibility that structural variability in the right SLF is relevant for SWM, nor do they imply significant lateralization of the effects. In the present study, we performed analyses to determine whether the association of SWM performance with left SLF FA was likely to be mediated by FA in the right SLF. No such mediating effect was observed, and our results suggest that left SLF FA exhibits an independent association with SWM not redundant with, or mediated by, a relationship with FA in the right hemisphere tract. We note that Nagy et al. (2004) also found a significant correlation between SWM performance and FA in the genu of the corpus callosum after controlling for age, a finding we also observed in the effect-size map (Figure 3).

Being one of the major fiber bundles connecting fronto-parietal regions the SLF is likely implicated in high-order cognitive processing and increased FA values have been associated with verbal abilities (Tamnes et al., 2010; Gold, Powell, Xuan, Jiang, & Hardy, 2007) and arithmetic skills (Tsang et al., 2009) in regions corresponding to the left SLF. Further, a DTI study found verbal working memory performance in schizophrenia patients and healthy participants to be correlated with FA in left SLF (Karlsgodt et al., 2008). Moreover, initial findings from DTI studies

in psychiatric populations have observed reduced FA values in left and/or right SLF, among other white matter regions, in major depressive disorder (Zou et al., 2008), schizophrenia (Szeszko et al., 2008; Mitelman et al., 2007), and attention deficit/hyperactivity disorder (Hamilton et al., 2008).

TBSS improves intersubject registration of brain fiber tracts relative to prior methods for performing spatial normalization of FA images (Smith et al., 2006), and the method obviates the need for extensive spatial smoothing. Thus, the use of TBSS in the present study aimed to increase the sensitivity of our ROI approach relative to ROI methods used in previous DTI studies in children. We averaged FA over the segments of the tract skeleton that corresponded to the expected location of the targeted tract after applying TBSS to align the tracts across subjects. This was considered to be a more objective way of estimating FA within a comparable portion of the tract within each individual than either subjective (manual) delineation of regions within the white matter or a voxel-wise approach. However, the method produces only an approximation of FA in the targeted tract, and in future studies, it may be possible to use better validated tractography methods that define the tracts on the basis of connectivity or new methods using probabilistic atlases (Hagler et al., 2009) to increase validity and reliability.

The results of the exploratory analyses of the parallel ($\lambda_{\parallel}$) and perpendicular ($\lambda_{\perp}$) diffusivities in left SLF may shed some light on possible factors mediating the observed variability in left SLF FA. Only the left SLF $\lambda_{\perp}$ was predictive of SWM scores after adjusting for age. No effects were observed with the measures of $\lambda_{\parallel}$. This suggests that the increases in SLF FA associated with better SWM performance are primarily attributable to the decreases in $\lambda_{\perp}$. Several factors have been linked to variability in $\lambda_{\perp}$ (Schwartz et al., 2005; Beaulieu, 2002). A study of diffusion parameters in myelin-deficient rats and age-matched controls demonstrated a significant but modest decrease in diffusion anisotropy in the unmyelinated spinal cord relative to control values. Furthermore, the decrease in anisotropy in the unmyelinated spinal cord was mainly due to increased $\lambda_{\perp}$ (Gulani, Webb, Duncan, & Lauterbur, 2001). In a study of the effects of retinal ischemia in mice, gradual decrease in relative anisotropy was found in the optic nerve. The decrease in anisotropy was, at first, associated with early axonal degeneration of the optic nerve seen as decreased $\lambda_{\parallel}$ with no detectable changes in $\lambda_{\perp}$, followed by later demyelination of the optic nerve associated with increases in $\lambda_{\perp}$ (Song et al., 2003). The results from these studies suggest that the observed decreases in left SLF $\lambda_{\perp}$ associated with improved SWM performance could be due to the degree of myelination of the fiber tract. Age-related FA increases in fiber tracts have been linked to decreases in $\lambda_{\perp}$ in previous studies (Lebel et al., 2008). However, other tissue parameters should be taken into account when interpreting FA and $\lambda_{\perp}$ such as axonal density, diameter and spacing, fiber packing, number of axons, extracellular volume fraction, and tract geometry (Schwartz et al., 2005; Beaulieu, 2002).

As mentioned earlier, these findings suggest that even among children of the same age, higher FA in left SLF is associated with better SWM performance. Many questions remain about what such age-adjusted variability in FA might represent. It may reflect individual differences in trajectories of fiber tract development, that is, differences in the phase of SLF development among children of similar age. Alternatively, it could represent individual differences in the structure of fiber tracts (perhaps reflecting differences in intracortical connectivity) that emerge earlier during brain development and remain stable in spite of superimposed biological changes associated with development. This is plausible because individual differences in behavioral performance have been associated with FA variability in adults (Gold et al., 2007; Wolbers, Schoell, & Buchel, 2006) as well as in children.

It is also possible that the fiber tract parameters are influenced dynamically, perhaps in association with activity levels in the neural circuits. In a DTI study comparing preterm infants to full-term infants at term equivalent age, we found that preterm infants exhibited higher FA values in the sagittal stratum, possibly as a result of increased sensorimotor stimulation in the extrauterine relative to the intrauterine environment (Gimenez et al., 2008). Further, a recent DTI study of adults examined changes in FA values before and after 2 months of training on three working memory tasks (including an SWM task). This study observed a positive correlation between amount of training and FA in a cluster adjacent to the intraparietal sulcus (Takeuchi et al., 2010). Thus, the differences measured in the present study could reflect variability in the experiences and learning of the children. Further environmental factors such as diet, exercise, and sleep could perhaps also influence individual brain maturation trajectories, although the relationships we observed did not appear to reflect global brain effects. Finally, genetic variability and interactions between genotype and environmental factors may play a role in mediating individual differences in left SLF FA and SWM skills.

In conclusion, SWM performance in children is associated with variability in left SLF FA and $\lambda_{\perp}$ that is not statistically attributable to age, and the relationship does not appear to reflect behavioral effects of global white matter development. Children of similar age may vary in the phase of maturation in the left SLF, and this variability may mediate the observed associations with SWM ability. Alternatively, the associations could be mediated by other sources of variability in the structure of the underlying fronto-parietal connections. Longitudinal observations may help to elucidate the meaning and implications of these associations.

Acknowledgments

The Danish Medical Research Council, The Lundbeck Foundation, and the University of Copenhagen's Research Priority Area Body and Mind are acknowledged for financial support.

Reprint requests should be sent to Martin Vestergaard or Kathrine Skak Madsen, MR-Department, Danish Research Centre for Magnetic Resonance, Copenhagen University Hospital, Section 340, Hvidovre, Kettegaard Allé 30, 2650 Hvidovre, Denmark, or via e-mail: martinvh@drcmr.dk; kathrine@drcmr.dk.

REFERENCES

Andersson, J. L., Hutton, C., Ashburner, J., Turner, R., & Friston, K. (2001). Modeling geometric deformations in EPI time series. *Neuroimage, 13,* 903–919.

Andersson, J. L. R., Jenkinson, M., & Smith, S. (2007). *Non-linear registration, aka spatial normalisation* (FMRIB Tech. Rep. No. TR07JA2). Retrieved from www.fmrib.ox.ac.uk/analysis/techrep.

Baddeley, A. (1981). The concept of working memory—A view of its current state and probable future-development. *Cognition, 10,* 17–23.

Basser, P. J., Mattiello, J., & LeBihan, D. (1994). MR diffusion tensor spectroscopy and imaging. *Biophysical Journal, 66,* 259–267.

Beaulieu, C. (2002). The basis of anisotropic water diffusion in the nervous system—A technical review. *NMR in Biomedicine, 15,* 435–455.

Cavada, C., & Goldman-Rakic, P. S. (1991). Topographic segregation of corticostriatal projections from posterior parietal subdivisions in the macaque monkey. *Neuroscience, 42,* 683–696.

Chafee, M. V., & Goldman-Rakic, P. S. (1998). Matching patterns of activity in primate prefrontal area 8a and parietal area 7ip neurons during a spatial working memory task. *Journal of Neurophysiology, 79,* 2919–2940.

Chang, L. C., Jones, D. K., & Pierpaoli, C. (2005). RESTORE: Robust estimation of tensors by outlier rejection. *Magnetic Resonance in Medicine, 53,* 1088–1095.

Cohen, J., & Cohen, P. (1983). *Applied multiple regression/correlation analysis for the behavioral sciences*. Hillsdale, NJ: Lawrence Erlbaum Associates.

Conklin, H. M., Luciana, M., Hooper, C. J., & Yarger, R. S. (2007). Working memory performance in typically developing children and adolescents: Behavioral evidence of protracted frontal lobe development. *Developmental Neuropsychology, 31,* 103–128.

Cook, P. A., Bai, Y., Nedjati-Gilani, S., Seunarine, K. K., Hall, M. G., Parker, G. J., et al. (2006). *Camino: Open-source diffusion-MRI reconstruction and processing*. 14th Scientific Meeting of the International Society for Magnetic Resonance in Medicine, Seattle, WA, USA.

Corbett, B. A., Constantine, L. J., Hendren, R., Rocke, D., & Ozonoff, S. (2009). Examining executive functioning in children with autism spectrum disorder, attention deficit hyperactivity disorder and typical development. *Psychiatry Research, 166,* 210–222.

De Luca, C. R., Wood, S. J., Anderson, V., Buchanan, J. A., Proffitt, T. M., Mahony, K., et al. (2003). Normative data from the Cantab: I. Development of executive function over the lifespan. *Journal of Clinical and Experimental Neuropsychology, 25,* 242–254.

du Boisgueheneuc, F., Levy, R., Volle, E., Seassau, M., Duffau, H., Kinkingnehun, S., et al. (2006). Functions of the left superior frontal gyrus in humans: A lesion study. *Brain, 129,* 3315–3328.

Duvernoy, H. M. (1999). *The human brain; surface, blood supply and three-dimensional section anatomy*. Wien: Springer.

Eluvathingal, T. J., Hasan, K. M., Kramer, L., Fletcher, J. M., & Ewing-Cobbs, L. (2007). Quantitative diffusion tensor tractography of association and projection fibers in normally developing children and adolescents. *Cerebral Cortex, 17,* 2760–2768.

Funahashi, S., Bruce, C. J., & Goldmanrakic, P. S. (1993). Dorsolateral prefrontal lesions and oculomotor delayed-response performance—Evidence for mnemonic scotomas. *Journal of Neuroscience, 13,* 1479–1497.

Giedd, J. N., Blumenthal, J., Jeffries, N. O., Castellanos, F. X., Liu, H., Zijdenbos, A., et al. (1999). Brain development during childhood and adolescence: A longitudinal MRI study. *Nature Neuroscience, 2,* 861–863.

Gimenez, M., Miranda, M. J., Born, A. P., Nagy, Z., Rostrup, E., & Jernigan, T. L. (2008). Accelerated cerebral white matter development in preterm infants: A voxel-based morphometry study with diffusion tensor MR imaging. *Neuroimage, 41,* 728–734.

Gold, B. T., Powell, D. K., Xuan, L., Jiang, Y., & Hardy, P. A. (2007). Speed of lexical decision correlates with diffusion anisotropy in left parietal and frontal white matter: Evidence from diffusion tensor imaging. *Neuropsychologia, 45,* 2439–2446.

Goldberg, M. C., Mostofsky, S. H., Cutting, L. E., Mahone, E. M., Astor, B. C., Denckla, M. B., et al. (2005). Subtle executive impairment in children with autism and children with ADHD. *Journal of Autism and Developmental Disorders, 35,* 279–293.

Goldman, P. S., & Rosvold, H. E. (1970). Localization of function within dorsolateral prefrontal cortex of rhesus monkey. *Experimental Neurology, 27,* 291–304.

Gulani, V., Webb, A. G., Duncan, I. D., & Lauterbur, P. C. (2001). Apparent diffusion tensor measurements in myelin-deficient rat spinal cords. *Magnetic Resonance in Medicine, 45,* 191–195.

Hagler, D. J., Jr., Ahmadi, M. E., Kuperman, J., Holland, D., McDonald, C. R., Halgren, E., et al. (2009). Automated white-matter tractography using a probabilistic diffusion tensor atlas: Application to temporal lobe epilepsy. *Human Brain Mapping, 30,* 1535–1547.

Hamilton, L. S., Levitt, J. G., O'Neill, J., Alger, J. R., Luders, E., Phillips, O. R., et al. (2008). Reduced white matter integrity in attention-deficit hyperactivity disorder. *NeuroReport, 19,* 1705–1708.

Jansons, K. M., & Alexander, D. C. (2003). Persistent angular structure: New insights from diffusion MRI data. Dummy version. *Information Processing in Medical Imaging, 18,* 672–683.

Jernigan, T. L., Gamst, A. C., Fennema-Notestine, C., & Ostergaard, A. L. (2003). More "mapping" in brain mapping: Statistical comparison of effects. *Human Brain Mapping, 19,* 90–95.

Jernigan, T. L., Trauner, D. A., Hesselink, J. R., & Tallal, P. A. (1991). Maturation of human cerebrum observed in vivo during adolescence. *Brain, 114,* 2037–2049.

Jovicich, J., Czanner, S., Greve, D., Haley, E., van der Kouwe, A., Gollub, R., et al. (2006). Reliability in multi-site structural MRI studies: Effects of gradient non-linearity correction on phantom and human data. *Neuroimage, 30,* 436–443.

Karlsgodt, K. H., van Erp, T. G., Poldrack, R. A., Bearden, C. E., Nuechterlein, K. H., & Cannon, T. D. (2008). Diffusion tensor imaging of the superior longitudinal fasciculus and working memory in recent-onset schizophrenia. *Biological Psychiatry, 63,* 512–518.

Klingberg, T., Forssberg, H., & Westerberg, H. (2002). Increased brain activity in frontal and parietal cortex underlies the development of visuospatial working memory capacity during childhood. *Journal of Cognitive Neuroscience, 14,* 1–10.

Koch, G., Oliveri, M., Torriero, S., Carlesimo, G. A., Turriziani, P., & Caltagirone, C. (2005). rTMS evidence of different delay and decision processes in a fronto-parietal neuronal network activated during spatial working memory. *Neuroimage, 24,* 34–39.

Lebel, C., Walker, L., Leemans, A., Phillips, L., & Beaulieu, C. (2008). Microstructural maturation of the human brain from childhood to adulthood. *Neuroimage, 40,* 1044–1055.

Leung, H. C., Oh, H., Ferri, J., & Yi, Y. J. (2007). Load response functions in the human spatial working memory circuit during location memory updating. *Neuroimage, 35,* 368–377.
Lycke, C., Specht, K., Ersland, L., & Hugdahl, K. (2008). An fMRI study of phonological and spatial working memory using identical stimuli. *Scandinavian Journal of Psychology, 49,* 393–401.
Madsen, K. S., Baare, W. F., Vestergaard, M., Skimminge, A., Ejersbo, L. R., Ramsoy, T. Z., et al. (2010). Response inhibition is associated with white matter microstructure in children. *Neuropsychologia, 48,* 854–862.
Mitelman, S. A., Torosjan, Y., Newmark, R. E., Schneiderman, J. S., Chu, K. W., Brickman, A. M., et al. (2007). Internal capsule, corpus callosum and long associative fibers in good and poor outcome schizophrenia: A diffusion tensor imaging survey. *Schizophrenia Research, 92,* 211–224.
Mori, S., Wakana, S., Nagae-Poetscher, L. M., & van Zijl, P. C. M. (2005). *MRI atlas of human white matter* (1st ed.). Amsterdam: Elsevier.
Muri, R. M., Gaymard, B., Rivaud, S., Vermersch, A., Hess, C. W., & Pierrot-Deseilligny, C. (2000). Hemispheric asymmetry in cortical control of memory-guided saccades. A transcranial magnetic stimulation study. *Neuropsychologia, 38,* 1105–1111.
Nagy, Z., Westerberg, H., & Klingberg, T. (2004). Maturation of white matter is associated with the development of cognitive functions during childhood. *Journal of Cognitive Neuroscience, 16,* 1227–1233.
Nichols, T. E., & Holmes, A. P. (2002). Nonparametric permutation tests for functional neuroimaging: A primer with examples. *Human Brain Mapping, 15,* 1–25.
Niogi, S. N., & McCandliss, B. D. (2006). Left lateralized white matter microstructure accounts for individual differences in reading ability and disability. *Neuropsychologia, 44,* 2178–2188.
Olesen, P. J., Nagy, Z., Westerberg, H., & Klingberg, T. (2003). Combined analysis of DTI and fMRI data reveals a joint maturation of white and grey matter in a fronto-parietal network. *Brain Research, Cognitive Brain Research, 18,* 48–57.
Oliveri, M., Turriziani, P., Carlesimo, G. A., Koch, G., Tomaiuolo, F., Panella, M., et al. (2001). Parieto-frontal interactions in visual-object and visual-spatial working memory: Evidence from transcranial magnetic stimulation. *Cerebral Cortex, 11,* 606–618.
Owen, A. M., McMillan, K. M., Laird, A. R., & Bullmore, E. (2005). N-back working memory paradigm: A meta-analysis of normative functional neuroimaging. *Human Brain Mapping, 25,* 46–59.
Owen, A. M., Morris, R. G., Sahakian, B. J., Polkey, C. E., & Robbins, T. W. (1996). Double dissociations of memory and executive functions in working memory tasks following frontal lobe excisions, temporal lobe excisions or amygdalo–hippocampectomy in man. *Brain, 119,* 1597–1615.
Paus, T., Collins, D. L., Evans, A. C., Leonard, G., Pike, B., & Zijdenbos, A. (2001). Maturation of white matter in the human brain: A review of magnetic resonance studies. *Brain Research Bulletin, 54,* 255–266.
Petrides, M., & Pandya, D. N. (2006). Efferent association pathways originating in the caudal prefrontal cortex in the macaque monkey. *Journal of Comparative Neurology, 498,* 227–251.
Reese, T. G., Heid, O., Weisskoff, R. M., & Wedeen, V. J. (2003). Reduction of eddy-current-induced distortion in diffusion MRI using a twice-refocused spin echo. *Magnetic Resonance in Medicine, 49,* 177–182.
Schwartz, E. D., Cooper, E. T., Fan, Y., Jawad, A. F., Chin, C. L., Nissanov, J., et al. (2005). MRI diffusion coefficients in spinal cord correlate with axon morphometry. *NeuroReport, 16,* 73–76.
Schweinsburg, A. D., Nagel, B. J., & Tapert, S. F. (2005). fMRI reveals alteration of spatial working memory networks across adolescence. *Journal of the International Neuropsychological Society, 11,* 631–644.
Smith, S. M., Jenkinson, M., Johansen-Berg, H., Rueckert, D., Nichols, T. E., Mackay, C. E., et al. (2006). Tract-based spatial statistics: Voxelwise analysis of multi-subject diffusion data. *Neuroimage, 31,* 1487–1505.
Smith, S. M., Jenkinson, M., Woolrich, M. W., Beckmann, C. F., Behrens, T. E., Johansen-Berg, H., et al. (2004). Advances in functional and structural MR image analysis and implementation as FSL. *Neuroimage, 23*(Suppl. 1), S208–S219.
Snook, L., Paulson, L. A., Roy, D., Phillips, L., & Beaulieu, C. (2005). Diffusion tensor imaging of neurodevelopment in children and young adults. *Neuroimage, 26,* 1164–1173.
Song, S. K., Sun, S. W., Ju, W. K., Lin, S. J., Cross, A. H., & Neufeld, A. H. (2003). Diffusion tensor imaging detects and differentiates axon and myelin degeneration in mouse optic nerve after retinal ischemia. *Neuroimage, 20,* 1714–1722.
Sowell, E. R., Thompson, P. M., Leonard, C. M., Welcome, S. E., Kan, E., & Toga, A. W. (2004). Longitudinal mapping of cortical thickness and brain growth in normal children. *Journal of Neuroscience, 24,* 8223–8231.
Sowell, E. R., Trauner, D. A., Gamst, A., & Jernigan, T. L. (2002). Development of cortical and subcortical brain structures in childhood and adolescence: A structural MRI study. *Developmental Medicine & Child Neurology, 44,* 4–16.
Srimal, R., & Curtis, C. E. (2008). Persistent neural activity during the maintenance of spatial position in working memory. *Neuroimage, 39,* 455–468.
Szeszko, P. R., Robinson, D. G., Ashtari, M., Vogel, J., Betensky, J., Sevy, S., et al. (2008). Clinical and neuropsychological correlates of white matter abnormalities in recent onset schizophrenia. *Neuropsychopharmacology, 33,* 976–984.
Takeda, K., & Funahashi, S. (2007). Relationship between prefrontal task-related activity and information flow during spatial working memory performance. *Cortex, 43,* 38–52.
Takeuchi, H., Sekiguchi, A., Taki, Y., Yokoyama, S., Yomogida, Y., Komuro, N., et al. (2010). Training of working memory impacts structural connectivity. *Journal of Neuroscience, 30,* 3297–3303.
Tamnes, C. K., Ostby, Y., Walhovd, K. B., Westlye, L. T., Due-Tonnessen, P., & Fjell, A. M. (2010). Intellectual abilities and white matter microstructure in development: A diffusion tensor imaging study. *Human Brain Mapping, 31,* 1609–1625.
Tsang, J. M., Dougherty, R. F., Deutsch, G. K., Wandell, B. A., & Ben Shachar, M. (2009). Frontoparietal white matter diffusion properties predict mental arithmetic skills in children. *Proceedings of the National Academy of Sciences, U.S.A., 106,* 22546–22551.
Van Asselen, M., Kessels, R. P. C., Neggers, S. F. W., Kappelle, L. J., Frijns, C. J. M., & Postma, A. (2006). Brain areas involved in spatial working memory. *Neuropsychologia, 44,* 1185–1194.
Westerberg, H., Hirvikoski, T., Forssberg, H., & Klingberg, T. (2004). Visuo-spatial working memory span: A sensitive measure of cognitive deficits in children with ADHD. *Child Neuropsychology, 10,* 155–161.
Wolbers, T., Schoell, E. D., & Buchel, C. (2006). The predictive value of white matter organization in posterior parietal cortex for spatial visualization ability. *Neuroimage, 32,* 1450–1455.
Zou, K., Huang, X. Q., Li, T., Gong, Q. Y., Li, Z., Luo, O. Y., et al. (2008). Alterations of white matter integrity in adults with major depressive disorder: A magnetic resonance imaging study. *Journal of Psychiatry & Neuroscience, 33,* 525–530.